Thermodynamic properties of thin films of superfluid ^{3}He-*A*

A. B. Vorontsov and J. A. Sauls
Department of Physics and Astronomy, Northwestern University, Evanston, Illinois 60208, USA
(Received 1 April 2003; published 22 August 2003)

The pairing correlations in superfluid ^{3}He are strongly modified by quasiparticle scattering off a surface or an interface. We present theoretical results and predictions for the order parameter, the quasiparticle excitation spectrum, and the free energy for thin films of superfluid ^{3}He. Both specular and diffuse scatterings by a substrate are considered, while the free surface is assumed to be a perfectly reflecting specular boundary. The results are based on self-consistent calculations of the order parameter and quasiparticle excitation spectrum at zero pressure. We obtain results for the phase diagram, free energy, entropy, and specific heat of thin films of superfluid^{3}He.

DOI: 10.1103/PhysRevB.68.064508 PACS number(s): 67.57.Bc, 67.57.Np

I. INTRODUCTION

The superfluid phases of bulk ^{3}He are condensates of *p*-wave, spin-triplet Cooper pairs. The order parameters describing the *A* and *B* phases spontaneously break orbital- and spin-rotational symmetries, as well as discrete symmetries of space and time inversion, of the normal Fermi-liquid phase of ^{3}He.[1] Pairing transitions of this type are called ''unconventional,'' and such systems exhibit novel phenomena associated with the spontaneously broken symmetries of the order parameter. A generic feature of superfluids with an unconventional order parameter is their sensitivity to scattering by impurities, defects, and boundaries. Scattering of quasiparticles by these objects leads to the suppression of the order parameter (pair breaking) and suppression of the superfluid transition as well as more subtle physical effects associated with the interplay of scattering and particle-hole coherence in the superfluid state. These effects persist over several coherence lengths, which for ^{3}He is $\xi_0 = \hbar v_f/2\pi k_B T_c \simeq 10^2$–$10^3$ Å. When ^{3}He is placed in a container or confined to a geometry with dimensions of the order of the coherence length scale the effects of the boundaries on the superfluid extend to all parts of the liquid, and there is in this sense no ''bulk'' phase.

Superfluidity of ^{3}He films was first reported in 1985.[2] Basic properties of superfluid films, such as the transition temperature, critical current, and superfluid density, have been measured in several laboratories.[3–5] Evidence of a presumed *A*-*B* phase transition has been reported by several groups, and a phase diagram has been constructed over a limited range of temperatures and film thickness.[6–8] Experimental observation of third sound in ^{3}He films also shows anomalies in the mode spectrum as a function of temperature and film thickness which cannot be accounted for within the hydrodynamic theory applicable to superfluid ^{4}He.[9] There are many open questions about the nature of the superfluid phases of ^{3}He in restricted geometries, including the identification of the superfluid order parameter and whether or not additional phases may be stabilized depending on the geometry and surface structure of the confining geometry.

Theoretical models and calculations of the surface structure and excitation spectrum of superfluid ^{3}He films are important for understanding both thermodynamic and nonequilibrium properties of superfluid films. Detailed comparison between theory and experiment for the temperature dependence of the heat capacity and entropy allows us to determine the density of states and low-lying excitations of the film. The heat capacity and entropy also enter the hydrodynamic equations that describe damping of low-frequency collective modes of superfluid films.

In this paper we report a theoretical study of superfluid ^{3}He in films with thickness ranging from $D \sim 1\xi_0$ to $15\xi_0$. This is a system similar to ^{3}He in a slab, except the ^{3}He is in general confined between different interfaces. Essential to any theory of superfluid ^{3}He in confined geometry are the boundary conditions that describe the effects of surface scattering on the pairing correlations, the quasiparticle spectrum, and quasiparticle distribution functions in the case of nonequilibrium properties.

Early theoretical investigations focused on pair breaking of the order parameter near a wall in the Ginzburg-Landau (GL) regime, and the implications of the pair-breaking effect on the boundary conditions for the hydrodynamic variables describing the *A* phase, in particular the ℓ vector.[10] These calculations, as well as calculations of the suppression of the transition temperature for superfluid ^{3}He in confined geometry,[11] were based on de Gennes' formulation of inhomogeneous superfluidity in terms of semiclassical correlation functions and a heuristic model of surface roughness which interpolated between specular and diffuse scattering of quasiparticles. More recent analyses based on the GL theory for the phase diagram and dynamical properties of ^{3}He in slabs and cylindrical pores are described in Refs. 12 and 13.

Extensions of surface pair-breaking calculations beyond the GL limit require a more detailed theoretical formulation of inhomogeneous states of superfluid ^{3}He. The most powerful theory of superfluid ^{3}He is based on the quasiclassical transport equations.[14–16] This theory is the natural extension of Landau's theory of normal Fermi liquids to include BCS pairing correlations. The quasiclassical theory is applicable to a broad range of phenomena and nonequilibrium states of inhomogeneous ^{3}He. The central objects of the quasiclassical theory are the propagators that describe both the quasiparticle excitations of the condensed phases and the correlated pairs that form the condensate. Theoretical calculations based on the quasiclassical theory for the surface order parameter and excitation spectrum near a wall or interface require boundary conditions for the quasiclassical propagators,

 ©2003 The American Physical Society

generally formulated from scattering theory and a specific model for the surface or interface.

Boundary conditions describing reflection from an atomically rough surface were developed by Buchholtz and Rainer[17] and implemented in the form of the randomly rippled wall (RRW) approximation for ^{3}He-B.[18,19] Alternative formulations of diffuse boundary conditions were implemented by Zhang *et al.*[20] based on scattering from a thin layer of atomic-size impurities coating an otherwise smooth surface and by Thuneberg *et al.*[21] based on scattering from a distribution of ''randomly oriented mirror'' (ROM) surfaces. Boundary conditions describing rough surfaces which are neither perfectly specular nor fully diffuse were developed by Nagai[22] in terms of a random S matrix. In the diffuse scattering limit the results of Ref. 23 for the order parameter suppression in ^{3}He-B agree well with those obtained by Zhang *et al.*[20] based on the thin-dirty-layer (TDL) model.

We report a theoretical analysis of the structure, excitation spectrum, and thermodynamic properties of superfluid ^{3}He films. The free surface is modeled as a specular surface, and the film resides on a substrate that we assume is atomically rough. We model the scattering of quasiparticles by the substrate by introducing a thin layer of atomic-size impurities randomly distributed on the surface (TDL model). The width d of the impurity layer is assumed to be much less than the superfluid coherence length, while the mean free path $l_{\rm imp}$ for quasiparticles propagating in the layer is much smaller than the width d. Thus, quasiparticles are strongly scattered inside the layer, but eventually scatter out of the layer at an angle uncorrelated with the incident trajectory. The limit $d/l_{\rm imp} \to \infty$ as $d \to 0$ describes a rough surface in the diffuse scattering limit. The specific formulation of the impurity model for diffuse scattering that we use was introduced by Ovchinnikov[24] for diffuse scattering from atomically rough metallic interfaces and was implemented for superfluid ^{3}He by Kopnin *et al.*[25]

We start from the quasiclassical theory of superfluidity with the boundary conditions described above and calculate the equilibrium properties of films of superfluid ^{3}He in the weak-coupling limit. We calculate suppression of the order parameter in the film, the quasiparticle density of states, superfluid free energy, entropy, and heat capacity. We are especially interested in films of thickness $D \lesssim D_{AB}$, where $D_{AB} \approx 9\xi_0$ marks the transition from the B-like phase for thicker films to the A-like phase for thinner films. It is in this region that most film experiments have been done. We find that because of diffuse scattering at one of the interfaces, a band of subgap states is formed and these states exist throughout the film for sufficiently thin films. The thermodynamic properties of the A phase are changed significantly by these gapless excitations.

The main sections of this paper are organized as follows. In Sec. II we describe the theoretical formulation of the quasiclassical transport equations and the boundary conditions that we use in our calculations. Results for the thin-film phase diagram are summarized in Sec. III. In Sec. IV we discuss the excitation spectrum for both specular and diffuse scattering, while in Sec. V we present the results for the free energy, entropy, and heat capacity of thin films. More technical aspects of computing the free energy and implementing the diffuse boundary condition in the Riccati formulation of the transport equations are included in appendixes.

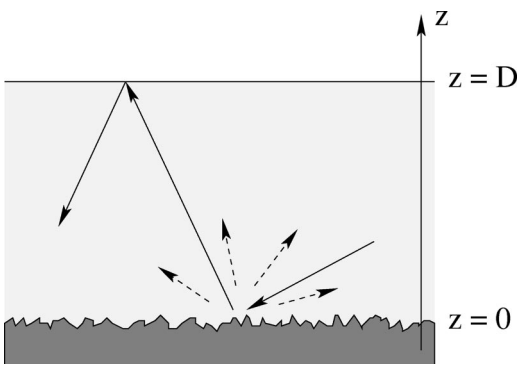

FIG. 1. A thin film of ^{3}He on an atomically rough substrate (at $z=0$) with a free surface ($z=D$) which is specular.

II. THEORETICAL MODEL

We assume that the ^{3}He film is on a substrate that is atomically rough on a scale much shorter than coherence length ξ_0. The film has a well-defined thickness D that is larger than the atomic scale. The free surface of the film is assumed to be atomically smooth; cf. Fig. 1. We assume that there is negligible evaporation and vapor above the film. Thus, the liquid in the film is essentially under zero pressure. In this model ^{3}He quasiparticles are specularly reflected at the free surface. We also assume that the film is invariant under translations and rotations in the plane of the film (xy plane),[38] and thus the physical properties of the film depend only on the z coordinate, which is normal to the substrate and the free surface.

The calculations we report were carried out using the quasiclassical theory for superfluid ^{3}He,[26] supplemented by boundary conditions for surface scattering at the vapor-liquid interface and film substrate. The central object of the quasiclassical theory is the propagator $\widehat{g}(\hat{\mathbf{p}},\mathbf{R};\varepsilon_m)$, which is a 4×4 Nambu matrix—denoted by a wide caret—in the combined particle-hole and spin spaces and is defined in terms of an integration of the full Nambu propagator,

$$\widehat{G}(\mathbf{p},\mathbf{R};\varepsilon_m) = \int_0^\beta d\tau e^{i\varepsilon_m\tau} \int d^3r e^{-i\mathbf{p}\cdot\mathbf{r}} - \langle \mathsf{T}_\tau \Psi(\mathbf{R}+\mathbf{r}/2,\tau)\overline{\Psi}(\mathbf{R}-\mathbf{r}/2,0)\rangle, \quad (1)$$

over a shell, $|v_f(p-p_f)| < \varepsilon_c \ll E_f$, in momentum space near the Fermi surface,

$$\widehat{g}(\hat{\mathbf{p}},\mathbf{R};\varepsilon_m) = \frac{1}{a}\int_{-\varepsilon_c}^{+\varepsilon_c} d\xi_{\mathbf{p}} \widehat{\tau}_3 \widehat{G}(\mathbf{p},\mathbf{R};\varepsilon_m). \quad (2)$$

The propagator is normalized by dividing by the weight of the quasiparticle pole in the spectral function a. We use the Matsubara representation to calculate equilibrium properties; the fermion Matsubara frequencies are $\varepsilon_m = (2m+1)\pi k_B T$. The four-component Nambu field operators are defined in

terms of the bare fermion field operators by $\Psi = (\psi_\uparrow, \psi_\downarrow, \psi_\uparrow^\dagger, \psi_\downarrow^\dagger)$ and $\overline{\Psi}(\mathbf{r},\tau) = \Psi^\dagger(\mathbf{r},-\tau)$.

For pure spin-triplet pairing the quasiclassical propagator $\widehat{g}$ may be parametrized in particle-hole space by 2×2 spin matrices for the diagonal (quasiparticle) and off-diagonal (Cooper pair) propagators,

$$\widehat{g} = \begin{pmatrix} \hat{g} & \hat{f} \\ \underline{\hat{f}} & \underline{\hat{g}} \end{pmatrix} = \begin{pmatrix} g + \hat{\boldsymbol{\sigma}}\cdot\mathbf{g} & (i\hat{\boldsymbol{\sigma}}\hat{\sigma}_y)\cdot\mathbf{f} \\ (i\hat{\sigma}_y\hat{\boldsymbol{\sigma}})\cdot\underline{\mathbf{f}} & \underline{g} + \hat{\boldsymbol{\sigma}}^{\mathrm{tr}}\cdot\underline{\mathbf{g}} \end{pmatrix}. \tag{3}$$

The 2×2 spin matrices are denoted by ordinary carets, e.g., $\hat{g}$. The spin vectors $\hat{\boldsymbol{\sigma}} = (\hat{\sigma}_x, \hat{\sigma}_y, \hat{\sigma}_z)$ are the Pauli matrices. One deviation from the matrix notation is $\hat{\mathbf{p}}$, which denotes a unit vector in the direction of the Fermi velocity $\mathbf{v}_f(\hat{\mathbf{p}}) = v_f\hat{\mathbf{p}}$. The components of the quasiclassical propagator are not all independent. The upper and lower particle-hole components are related by symmetries that follow from the fermion anticommutation relations

$$\begin{aligned} \underline{\hat{f}}(\hat{\mathbf{p}},\mathbf{R};\varepsilon_m) &= \hat{f}(-\hat{\mathbf{p}},\mathbf{R};\varepsilon_m)^* = -\hat{f}(\hat{\mathbf{p}},\mathbf{R};-\varepsilon_m)^\dagger, \\ \underline{\hat{g}}(\hat{\mathbf{p}},\mathbf{R};\varepsilon_m) &= \hat{g}(-\hat{\mathbf{p}},\mathbf{R};\varepsilon_m)^* = \hat{g}(-\hat{\mathbf{p}},\mathbf{R};-\varepsilon_m)^{\mathrm{tr}}, \end{aligned} \tag{4}$$

where $\hat{g}^{\mathrm{tr}}$ is the matrix transpose of $\hat{g}$.

The quasiclassical transport equation that governs the evolution of the quasiclassical propagator $\widehat{g}(\hat{\mathbf{p}},\mathbf{R};\varepsilon_m)$ is[14,26]

$$[i\varepsilon_m\widehat{\tau}_3 - \widehat{\Delta}(\hat{\mathbf{p}},\mathbf{R}), \widehat{g}(\hat{\mathbf{p}},\mathbf{R};\varepsilon_m)] + i\mathbf{v}_f(\hat{\mathbf{p}})\cdot\boldsymbol{\nabla}\widehat{g}(\hat{\mathbf{p}},\mathbf{R};\varepsilon_m) = 0, \tag{5}$$

with a constraint given by Eilenberger's normalization condition on $\widehat{g}$,

$$\widehat{g}(\hat{\mathbf{p}},\mathbf{R};\varepsilon_m)^2 = -\pi^2\widehat{1}. \tag{6}$$

We have omitted the Landau molecular field self-energy in the transport equation, and we consider the pairing self-energy $\widehat{\Delta}$ in the weak-coupling limit, which is a convenient choice for the order parameter. It is off diagonal in particle-hole space,

$$\widehat{\Delta} = \begin{pmatrix} 0 & \hat{\Delta} \\ \underline{\hat{\Delta}} & 0 \end{pmatrix} = \begin{pmatrix} 0 & i\hat{\boldsymbol{\sigma}}\hat{\sigma}_y\cdot\boldsymbol{\Delta} \\ i\hat{\sigma}_y\hat{\boldsymbol{\sigma}}\cdot\boldsymbol{\Delta}^* & 0 \end{pmatrix} \tag{7}$$

and parametrized by a spin-triplet order parameter defined by the vector $\boldsymbol{\Delta}(\hat{\mathbf{p}},\mathbf{R})$. In the weak-coupling limit the order parameter is determined by the off-diagonal pair amplitude $\mathbf{f}(\hat{\mathbf{p}},\mathbf{R};\varepsilon_m)$ from the gap equation

$$\boldsymbol{\Delta}(\hat{\mathbf{p}},\mathbf{R}) = T\sum_m^{|\varepsilon_m|<\varepsilon_c}\int\frac{d\Omega_{\hat{\mathbf{p}}'}}{4\pi}V(\hat{\mathbf{p}},\hat{\mathbf{p}}')\mathbf{f}(\hat{\mathbf{p}}',\mathbf{R};\varepsilon_m), \tag{8}$$

where $V(\hat{\mathbf{p}},\hat{\mathbf{p}}')$ is the interaction in the spin-triplet pairing channel. For pure p-wave pairing we retain only the attractive $\ell = 1$ interaction $V = 3V_1\hat{\mathbf{p}}\cdot\hat{\mathbf{p}}'$. The cutoff ε_c and interaction V_1 are not measurable, but they are related to the bulk transition temperature by

$$\frac{1}{V_1} = \pi T_c\sum_m^{|\varepsilon_m|<\varepsilon_c}\frac{1}{|\varepsilon_m|} \approx \ln\frac{1.13\varepsilon_c}{T_c}, \tag{9}$$

which is used to eliminate the cutoff and pairing interaction in favor of the measured bulk transition temperature T_c.

The order parameter must be determined self-consistently with the solution of the transport equation for the propagator. This procedure and the quasiclassical transport equation can be simplified by introducing a parametrization for the propagator that satisfies the normalization condition by construction and reduces the number of independent components,

$$\widehat{g} = -i\pi\widehat{N}\begin{pmatrix} \hat{1}+\hat{a}\underline{\hat{a}} & 2\hat{a} \\ -2\underline{\hat{a}} & -\hat{1}-\underline{\hat{a}}\hat{a} \end{pmatrix}, \tag{10}$$

where the prefactor is given by

$$\widehat{N} = \begin{pmatrix} (\hat{1}-\hat{a}\underline{\hat{a}})^{-1} & 0 \\ 0 & (\hat{1}-\underline{\hat{a}}\hat{a})^{-1} \end{pmatrix}. \tag{11}$$

The amplitudes $\hat{a}$ and $\underline{\hat{a}}$ are 2×2 matrices in spin space which obey matrix Ricatti equations[27–29]

$$\begin{aligned} i\mathbf{v}_f\cdot\boldsymbol{\nabla}\hat{a} + 2i\varepsilon_m\hat{a} - \hat{a}\underline{\hat{\Delta}}\hat{a} + \hat{\Delta} &= 0, \\ i\mathbf{v}_f\cdot\boldsymbol{\nabla}\underline{\hat{a}} - 2i\varepsilon_m\underline{\hat{a}} - \underline{\hat{a}}\hat{\Delta}\hat{a} + \underline{\hat{\Delta}} &= 0. \end{aligned} \tag{12}$$

We refer to $\hat{a}$ and $\underline{\hat{a}}$ as the Ricatti amplitudes. The two Ricatti amplitudes are related to the particlelike and holelike projections of the off-diagonal propagators,

$$\hat{a} = -(i\pi - \hat{g})^{-1}\hat{f}, \quad \underline{\hat{a}} = (i\pi + \underline{\hat{g}})^{-1}\underline{\hat{f}}, \tag{13}$$

where the projection operators for the particlelike ($\widehat{P}_+$) and holelike ($\widehat{P}_-$) sectors are given by

$$\widehat{P}_+ = \frac{1}{2}\left(1 + \frac{\widehat{g}}{-i\pi}\right), \quad \widehat{P}_- = \frac{1}{2}\left(1 - \frac{\widehat{g}}{-i\pi}\right). \tag{14}$$

For the case of spin-triplet pairing in zero field these amplitudes can be parametrized as

$$\hat{a} = (i\hat{\boldsymbol{\sigma}}\cdot\hat{\sigma}_y)\cdot\mathbf{a} \quad \text{and} \quad \underline{\hat{a}} = (i\hat{\sigma}_y\hat{\boldsymbol{\sigma}})\cdot\underline{\mathbf{a}}. \tag{15}$$

The Ricatti amplitudes are also related to each other by a symmetry that follows from symmetry relations for the propagators in Eqs. (4),

$$\hat{a}(\hat{\mathbf{p}},\mathbf{R};\varepsilon_m)^* = \underline{\hat{a}}(-\hat{\mathbf{p}},\mathbf{R};\varepsilon_m). \tag{16}$$

The Ricatti equations are easily integrated numerically, are numerically stable, and provide a more efficient approach to solving the quasiclassical transport equations than the "explosion method."[30] Equations (12) are solved by integration along classical trajectories—forward for $\hat{a}$ and backward for $\underline{\hat{a}}$—starting from an initial value. The Ricatti equations must be supplemented by boundary conditions at the two interfaces. We do not have a bulk region in the ^{3}He film, so generally we start from an arbitrary initial value at the free surface and compute along a classical trajectory with mul-

tiple reflections until the Ricatti amplitude at the surface converges. The integration procedure is described in more detail in Appendix A.

The boundary conditions for the Ricatti amplitudes at the two interfaces are obtained from boundary conditions for the quasiclassical propagators. Specular reflection at the free surface requires matching of the propagators at the free surface for two trajectories, $\hat{\mathbf{p}}$ and $\underline{\hat{\mathbf{p}}}$, which are related by $\underline{\hat{\mathbf{p}}}=\hat{\mathbf{p}}-2\hat{\mathbf{n}}(\hat{\mathbf{n}}\cdot\hat{\mathbf{p}})$,

$$\widehat{g}(\hat{\mathbf{p}},D;\varepsilon_m)=\widehat{g}(\underline{\hat{\mathbf{p}}},D;\varepsilon_m). \tag{17}$$

Then the Ricatti amplitudes are also matched at the surface in the same way,

$$\hat{a}(\hat{\mathbf{p}},D;\varepsilon_m)=\hat{a}(\underline{\hat{\mathbf{p}}},D;\varepsilon_m), \tag{18}$$

$$\underline{\hat{a}}(\hat{\mathbf{p}},D;\varepsilon_m)=\underline{\hat{a}}(\underline{\hat{\mathbf{p}}},D;\varepsilon_m). \tag{19}$$

The boundary condition for the quasiclassical propagator at an atomically rough surface is more complicated. A physical model for an atomically rough surface is provided by a TDL model for surface roughness obtained by coating a specular surface with a layer (of thickness d) of randomly distributed impurities characterized by a mean free path of $l_{\rm imp}$.[31] In the TDL model the ratio $\rho=d/l_{\rm imp}$ describes the degree of surface roughness. For $\rho=0$ we recover a specularly reflecting surface, while $\rho\to\infty$ corresponds to the fully diffuse surface. In the fully diffuse limit we implement Ovchinikov's boundary condition, which is a special case of the diffuse limit of the TDL boundary condition. The Ovchinnikov boundary condition requires self-consistent determination of the Green's function at the diffuse surface, $\widehat{g}(\hat{\mathbf{p}},0;\varepsilon_m)$. For outgoing trajectories ($\hat{\mathbf{p}}_z>0$) the boundary condition for the Ricatti amplitude is

$$\hat{a}(\hat{\mathbf{p}},0)=-(i\pi-\hat{g}_{\rm TDL})^{-1}\hat{f}_{\rm TDL}, \tag{20}$$

where $\hat{g}_{\rm TDL}(\varepsilon_m)$ and $\hat{f}_{\rm TDL}(\varepsilon_m)$ are the propagators deep in the dirty layer and which are related to the surface propagator by

$$\widehat{g}_{\rm TDL}(\varepsilon_m)=\int_{\substack{\hat{p}_z>0\\ \hat{p}_z<0}}\frac{d\Omega_{\hat{\mathbf{p}}}}{\pi}|\hat{p}_z|\,\widehat{g}(\hat{\mathbf{p}},0;\varepsilon_m). \tag{21}$$

We give a short derivation of this boundary condition in Appendix A.

Order parameter

We consider two possible phases in superfluid ^{3}He films that have the same or nearly the same symmetry, as the A and B phases of bulk superfluid ^{3}He when one restricts the orbital symmetry group to SO(2). The order parameter for the B-like phase is of the form

$$\mathbf{\Delta}_B=(\Delta_\parallel(z)\hat{p}_x,\Delta_\parallel(z)\hat{p}_y,\Delta_\perp(z)\hat{p}_z), \tag{22}$$

while that for the A-like ("axial") phase is given by

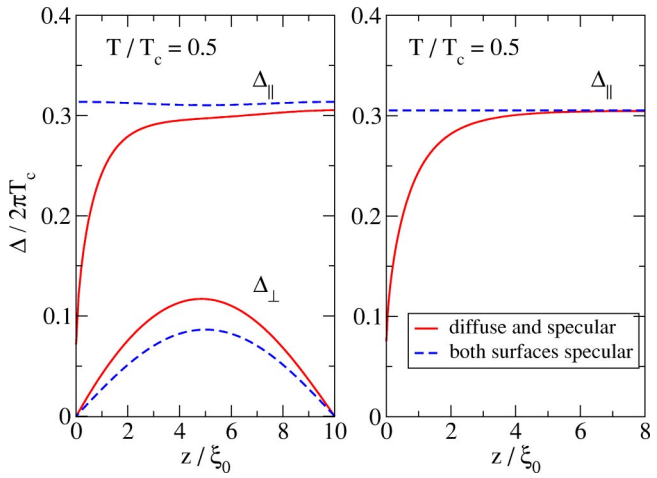

FIG. 2. The order parameters for the B-like and A-like phases of ^{3}He in a thin film. The coherence length $\xi_0=\hbar v_f/2\pi k_B T_c$ is approximately equal to 73 nm at zero pressure.

$$\mathbf{\Delta}_A=(0,0,\Delta_\parallel(z)(\hat{p}_x+i\hat{p}_y)), \tag{23}$$

where $\parallel$ and $\perp$ refer to orbital motion, characterized by the direction of the relative momentum $\hat{\mathbf{p}}$, parallel and perpendicular to the surfaces of the film. The *planar* phase is a special case of the B phase with $\Delta_\perp=0$. For the A-like phase we have $\mathbf{\Delta}_A\|\boldsymbol{\ell}=\hat{\mathbf{z}}$ in order to minimize the nuclear dipolar energy. For the B phase the order parameter in Eq. (22) is multiplied by a spin-orbit rotation matrix $\mathcal{R}(\mathbf{n},\vartheta)$, which is fixed by the dipole energy.

The spatial profiles of the order parameter components are shown in Fig. 2 for both the B-like (left panel) and A-like (right panel) phases. The dashed lines correspond to a film with two specular surfaces, while the solid lines represent a film with diffuse scattering from a substrate at $z=0$ and specular reflection from the free surface.

The orbital components of the order parameter that are perpendicular to the film interface, $\Delta_\perp$, are suppressed at both interfaces. This suppression is related to the change of sign of $\Delta_\perp\hat{p}_z$ when a quasiparticle is reflected by the surface. The parallel component $\Delta_\parallel$ is suppressed by diffuse scattering at the substrate in both phases. In the B phase $\Delta_\perp$ is slightly increased for diffuse scattering because some of the spectral weight that is lost from $\Delta_\parallel$ is transferred to $\Delta_\perp$.

The orbital structure of the order parameter for the A phase leads to a simplification for the boundary condition at the diffuse substrate. If we parametrize the off-diagonal component of $\hat{g}$ by

$$\mathbf{f}=(0,0,f_\parallel(\hat{p}_z)(\hat{p}_x+i\hat{p}_y)), \tag{24}$$

then the angular integration in Eq. (21) gives $\hat{f}_{\rm TDL}=0$. Thus, we have an explicit value for the Ricatti amplitude $\hat{a}$ at that surface,

$$\hat{a}(\hat{\mathbf{p}},0;\varepsilon_m)=0,\quad \hat{p}_z>0. \tag{25}$$

The quasiclassical Green's function at $z=0$ is then

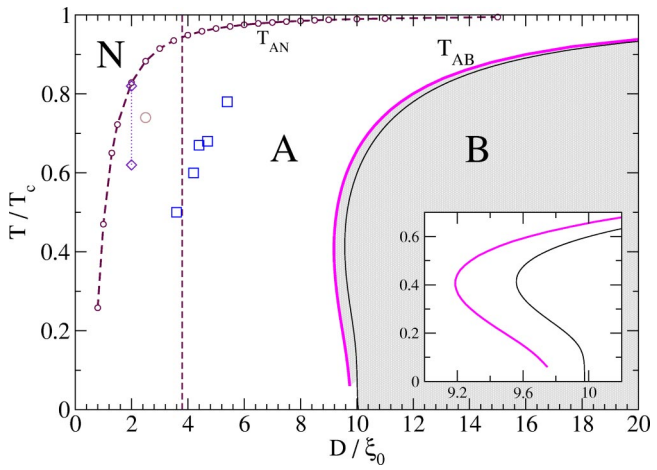

FIG. 3. Phase diagram for superfluid ^{3}He films. The thick solid line represents the *AB* transition for a film in contact with a rough substrate and a specular free surface. The thin solid line is the *AB* phase boundary for a film with two specular surfaces. The inset shows an enlarged portion of the *AB* phase boundary, where the second-order transition is reentrant, $A \rightarrow B \rightarrow A$, as a function of temperature. The dashed line shows the normal (*N*) to *A*-phase boundary, with suppression of the superfluid transition, $T_c^{\rm film} < T_c$, resulting from diffuse scattering by the substrate. The individual points correspond to observed anomalies in measurements that may indicate a phase transition in the superfluid film: (a) thin dashed line, anomaly in $\rho_s(T,D)$ (Ref. 7); (b) open squares, mode anomaly in third sound (Ref. 9); (c) open circle, flow anomaly (Ref. 5); (d) open diamonds, flow anomaly (Ref. 3).

$$\hat{g}(\hat{\mathbf{p}},0,\varepsilon_m) = -i\pi \begin{pmatrix} \hat{1} & 0 \\ -2\underline{\hat{a}} & -\hat{1} \end{pmatrix}, \quad \hat{p}_z > 0. \tag{26}$$

The boundary value in Eq. (25) speeds up numerical integration since the calculation of $\hat{a}(\hat{p}_z>0)$ and $\underline{\hat{a}}(\hat{p}_z<0)$ are now initial value problems; we start at $z=0$ with $\hat{a}(\hat{p}_z>0,0;\varepsilon_m)=0$, or $\underline{\hat{a}}(\hat{p}_z<0,0;\varepsilon_m)=0$ and integrate the Ricatti equations directly to obtain $\hat{a}(\hat{p}_z>0,z;\varepsilon_m)$ and $\underline{\hat{a}}(\hat{p}_z<0,z;\varepsilon_m)$.

III. PHASE DIAGRAM

At zero pressure bulk ^{3}He is in the superfluid *B* phase for temperatures below $T_c = 0.93$ mK. When we confine the superfluid to a slab between two surfaces or form a film on a substrate, we observe changes in the superfluid as we decrease the film thickness *D*. The phase diagram of ^{3}He in superfluid films, as far as it is known, is shown in Fig. 3. Several phase transition lines calculated theoretically are shown, as well as points indicating possible phase transitions based on anomalies in several experiments.

If one starts from the bulk superfluid *B* phase and then reduces the film thickness *D* at constant temperature, we expect to cross at least two phase boundaries. As *D* is reduced the perpendicular component $\Delta_\perp(z)$ is suppressed, and at a critical film thickness, $D_{AB}(T)$, $\Delta_\perp(z)$ vanishes. This signifies a transition to the *planar* phase with an order parameter of the form $\mathbf{\Delta}_{\rm P} = \Delta_\parallel(z)(\hat{p}_x,\hat{p}_y,0)$. The component $\Delta_\perp(z)$ vanishes continuously, so this transition is second order. In the weak-coupling limit the planar and axial phases are degenerate. However, in bulk ^{3}He strong-coupling corrections lower the free energy of the axial phase relative to the planar phase. Thus, if strong-coupling effects also stabilize the axial phase relative to the planar phase in a thin film, then the second-order transition from the *B* phase to the planar phase is preempted by a transition from the *B* phase to the axial *A* phase. Measurements of the heat capacity jump in bulk ^{3}He indicate that strong-coupling corrections are small at zero pressure; thus, the *AB* transition in the film is likely to be very weakly first order. With the exception of the possible fine structure of the phase diagram close to the second-order transition line $D_{AB}(T)$ and properties such as the latent heat of transition, calculations of the thermodynamic properties of thin films based on the weak-coupling approximation are expected to be accurate.

The perpendicular component of the order parameter is suppressed to zero even for a specular wall, so the *AB* transition occurs even in a film bounded by two specular surfaces. For a film on a rough substrate, the suppression of $\Delta_\parallel$ by diffuse scattering leads to a small enhancement of $\Delta_\perp(z)$. As a result the *B* to *A* transition requires slightly thinner films for a rough substrate. This result, although the detailed shape of the phase boundary is slightly different, agrees with the calculations reported by Nagato and Nagai[34] based on a different theoretical model for the surface roughness. However, NMR measurements[8] on thin slabs of superfluid ^{3}He show that the *AB* transition occurs at larger values of film thickness than predicted by the weak-coupling theory. This may indicate that the first-order *AB* phase boundary needs to be calculated with leading-order strong-coupling corrections included in the theory, even at zero pressure.

An interesting feature of the calculated weak-coupling *AB* phase boundary below $T/T_c \approx 0.4$ is shown in the inset of Fig. 3. For films in contact with either a specular or rough substrate the second-order phase boundary is reentrant as a function of temperature for a narrow range of film thicknesses. For example, for a film on a rough surface with $D \simeq 9.4\xi_0$, upon decreasing the temperature below $T_c^{\rm film}$ the *A* to *B* transition occurs at $T_{\rm AB} \approx 0.55 T_c$. As the temperature drops further a reentrant *B* to *A* transition occurs at $T_{BA} \simeq 0.23 T_c$. Whether or not this reentrance will survive strong-coupling corrections is not known. The reentrance may also signal that a translationally invariant *A* or *B* phase is unstable to the formation of an inhomogeneous phase with lower free energy. In any event the fine structure of the phase diagram at low temperatures near $D \simeq 9.5\xi_0$ and the possibility of new phases stabilized by strong-coupling corrections or which spontaneously break translation symmetry in the plane of the film is outside the scope of this paper.

For films that are thinner than $(9.5\text{–}10)\xi_0$ the planar or axial *A* phase is the stable phase relative to the *B*-like phase. For the purpose of calculating the thermodynamic properties we assume that strong-coupling corrections stabilize the *A* phase relative to the planar phase in the film; however, this is really an open question. Strong-coupling corrections to the free energy for phases with strong spatial variations, as occurs in thin films, have not been calculated, so the relative

stability of the planar and *A* phase in thin films is unknown, either theoretically or experimentally.

If the substrate were an ideal specularly reflecting surface, then the superfluid *A* phase would persist for film thicknesses approaching a few monolayers or until the Fermi-liquid properties and pairing interaction were modified by finite-size effects. But the pair-breaking effect of scattering off a rough substrate suppresses the transition temperature into the *A* phase, and at a film width $D_{AN}(T)$, which is substantially smaller than $D_{AB}(T)$, the superfluid *A* phase is destroyed. The calculated transition temperature for diffuse scattering is shown in Fig. 3. This phase boundary was calculated by identifying the temperature and film thickness where the order parameter vanishes. We also obtained the superfluid transition from the calculated free energy by a least-squares fit of the known Ginzburg-Landau form for the free energy, $a(T-T_c^{\rm film})^2$.

Calculations of the transition temperature in thin slabs of ^{3}He were carried out by Kjäldman *et al.* [11] using a linearized gap equation and de Gennes' formulation of the kernel in terms of the classical limit for the normal-state current-current correlation function.[10] Our calculations agree well with the results for a slab if we take into account that the width of the thin film of ^{3}He-*A* is equivalent to a ^{3}He-*A* slab of twice the width of the film.

It should be noted that the phases considered here, even for thin ^{3}He films, assume thicknesses $D \gg$ Å. We do not consider the two-dimensional (2D) limit of one or two atomic layers of ^{3}He atoms on the surface of a substrate. The properties of 2D superfluid ^{3}He, if it exists, are expected to be influenced by the reduced dimensionality. Ising-like as well as Kosterlitz-Thouless-type transitions are predicted for 2D superfluid ^{3}He-*A*.[32,33]

One additional note: observing the equilibrium phase boundaries may be complicated by metastability. Even though the planar phase—i.e., the *B* phase with $\Delta_\perp = 0$—and the axial *A* phase are degenerate in weak coupling, they are unrelated by symmetry and, therefore, separated by an energy barrier. Thus, once established, the axial *A* phase will be metastable with respect to the *B* phase. The calculation of the barrier and corresponding metastability lines in the phase diagram would provide an important result, but are outside the scope of this article.

IV. DENSITY OF STATES

Pair breaking by surface scattering leads to quasiparticle states below the gap. These excitations play an important role in the thermodynamic and transport properties of thin films of superfluid ^{3}He. The subgap excitations are surface Andreev bound states. The mechanism leading to their formation is closely related to the formation of bound states in the core of a vortex.[35] Andreev bound-state formation occurs when the order parameter changes sign or phase along a quasiparticle trajectory. In the case of surface scattering the incident and reflected trajectories generally correspond to very different order parameters; this is typically the case for an unconventional order parameter which breaks rotational symmetry.

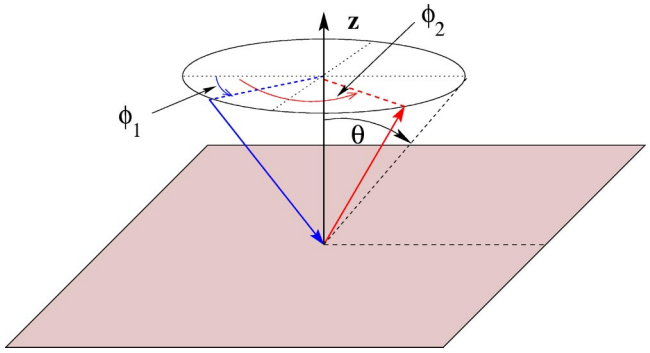

FIG. 4. Skew scattering by the substrate.

For example, consider the *B*-phase in contact with a specular surface. For an incident trajectory normal to the interface, $\hat{\mathbf{p}} \| \hat{\mathbf{z}}$, the *B*-phase order parameter changes sign upon reflection: i.e., $\mathbf{\Delta}(\hat{\underline{\mathbf{p}}}) = -\mathbf{\Delta}(\hat{\mathbf{p}})$ for $\hat{\mathbf{p}} \to \hat{\underline{\mathbf{p}}} = -\hat{\mathbf{p}}$. This sign change leads to a multiple Andreev reflection that generates a surface bound state at the Fermi level: i.e., $\varepsilon = 0$. For trajectories away from normal incidence the components of the *B*-phase order parameter corresponding to orbital motion in the plane are present and do not change sign upon reflection. As a result the surface Andreev bound state disperses as a function of the incident and reflected angles relative to the interface normal.

The bound-state energy dispersion can be calculated approximately by neglecting the suppression of the order parameter at the surface and assuming that surface scattering occurs on a cone defined by the angle θ from the *xy* plane—i.e., $(\theta, \phi_1) \to (\pi - \theta, \phi_2), \phi = \phi_2 - \phi_1$—as shown in Fig. 4. We then find bound-state poles in the retarded propagator, for either the *B* or *A* phase, given by

$$\varepsilon_b = \pm \Delta_\parallel \sin\theta \cos\frac{\phi}{2}. \tag{27}$$

The density of states (DOS) can be calculated once the order parameter and Landau molecular fields have been determined self-consistently. The most detailed information is contained in the angle-resolved local density of states, which is obtained from the diagonal component of the retarded quasiclassical propagator,

$$N(\hat{\mathbf{p}}, \mathbf{R}; \varepsilon) = -\frac{1}{\pi} \mathrm{Im}\, g^R(\hat{\mathbf{p}}, \mathbf{R}; \varepsilon), \tag{28}$$

where $g^R(\hat{\mathbf{p}}, \mathbf{R}; \varepsilon)$ is found by solving the quasiclassical transport equation for real energies: i.e., $i\varepsilon_m \to \varepsilon + i0^+$ and the known order parameter and molecular fields. The local density of states for the *B* phase near a wall shows quasiparticle states which develop below the bulk gap and are bound to the surface; i.e., their spectral weight vanishes a few coherence lengths away from the surface.

For example, the angle-resolved spectrum of superfluid ^{3}He-*B* near a specular surface, calculated numerically for a self-consistently determined order parameter, is shown in Fig. 5. For the specular reflection the position of the positive-energy surface bound state depends on the angle of the inci-

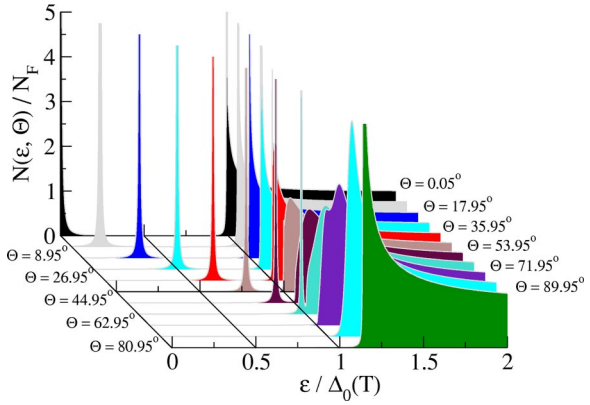

FIG. 5. The angle-resolved local DOS for the ^{3}He-B near a specular surface. The spectrum is calculated for $T=0.5T_c$. For clarity we have broadened the Andreev bound states with a width parameter of $\eta=10^{-3}\Delta_0$.

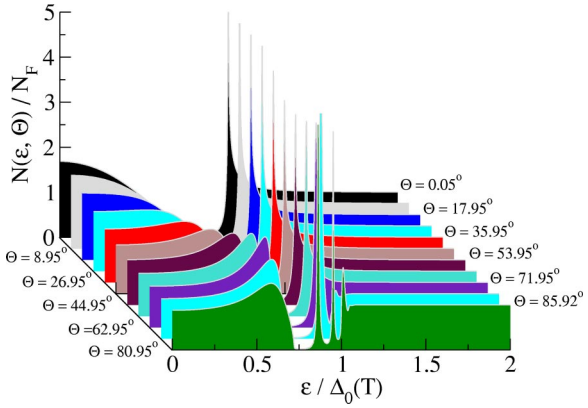

FIG. 6. The angle-resolved local DOS for the ^{3}He-B near a diffuse surface. The spectrum is calculated for $T=0.5T_c$. For clarity we have broadened the Andreev bound states near grazing incidence with a width parameter of $\eta=10^{-3}\Delta_0$.

dent trajectory, θ, approximately as $\varepsilon_b=\Delta_\parallel\sin\theta$. For normal incidence the bound state is at zero energy and disperses towards, eventually merging into, the continuum edge as the incident trajectory approaches grazing incidence. There is also a weak dispersion in the continuum edge reflecting the enhancement of $\Delta_\perp$ by surface scattering.

At an atomically rough surface diffuse scattering couples an incident trajectory to all outgoing trajectories. This leads to mixing of states with different energies and thus to a band of subgap states for a given incident trajectory as shown in Fig. 6. The suppression of $\Delta_\parallel$ for diffuse scattering also leads to the formation of additional subgap states bound by multiple Andreev reflection within the ''pair potential'' provided by the suppressed order parameter $\Delta_\parallel(z)$. These states appear only near grazing incidence and are weakly bound with energies just below the continuum edge.

Subgap states do not appear in ^{3}He-A at a specular wall since there is no change in phase of the order parameter for specular reflection when $\ell\|\hat{\mathbf{z}}$. Thus, all quasiparticle states belong to the continuum. This situation changes dramatically for a rough surface. Now there are scattering processes connecting an incident trajectory with a reflected trajectory that is at a skew angle $\phi\neq\pi$ in the xy plane (see Fig. 4). For ^{3}He-A the order parameter for a trajectory, $\hat{\mathbf{p}}=\cos\theta\hat{\mathbf{z}}+\sin\theta(\cos\phi\hat{\mathbf{x}}+\sin\phi\hat{\mathbf{y}})$, is $\mathbf{\Delta}_A(\hat{\mathbf{p}})=\hat{\mathbf{z}}\Delta_\parallel\sin\theta e^{i\phi}$. The change in phase of the order parameter upon skew scattering leads to strong pair breaking and the formation of subgap states. For the diffuse scattering the coupling of skew trajectories with all possible azimuthal angles generates a band of states which fill the subgap spectrum as shown in Fig. 7 for several incident trajectories.

The self-consistent spectrum calcuated numerically and shown in Fig. 7 is well described by the spectrum obtained by calculating the retarded propagator for a constant order parameter $\Delta_\parallel$ everywhere in the film. The spectrum is then determined entirely by the changes in the order parameter induced by diffuse scattering. The transport equation can be solved analytically with Ovchinnikov's boundary condition for the Riccati amplitudes. For the diagonal part of the quasiclassical propagator we obtain

$$g(\theta,z;\varepsilon_m)=-i\pi\left[1+\frac{1}{1+\dfrac{\varepsilon_m}{\Delta_\parallel^2\sin^2\theta}(\varepsilon_m+\omega\tanh[2\omega D/v_f\cos\theta])}\left(\frac{\cosh[2\omega(z-D)/v_f\cos\theta]}{\cosh[2\omega D/v_f\cos\theta]}-1\right)\right], \tag{29}$$

where $\omega^2=\Delta(\theta)^2+\varepsilon_m^2$ with $\Delta(\theta)=\Delta_\parallel\sin\theta$. We calculate the retarded propagator by analytic continuation to the real energy axis, $i\varepsilon_m\rightarrow\varepsilon+i0^+$. The result for the local density of states is then

$$N(\theta,z;\varepsilon)/N_f=1+\Theta(\varepsilon^2-\Delta(\theta)^2)\frac{1}{1-\dfrac{\varepsilon^2}{\Delta(\theta)^2}(1+\tan^2[2\omega D/v_f\cos\theta])}\left(\frac{\cos[2\omega(z-D)/v_f\cos\theta]}{\cos[2\omega D/v_f\cos\theta]}-1\right)$$

$$+\Theta(\Delta(\theta)^2-\varepsilon^2)\frac{1}{1-\dfrac{\varepsilon^2}{\Delta(\theta)^2}(1-\tanh^2[2\omega D/v_f\cos\theta])}\left(\frac{\cosh[2\omega(z-D)/v_f\cos\theta]}{\cosh[2\omega D/v_f\cos\theta]}-1\right), \tag{30}$$

where ω is now

$$\omega = \sqrt{|\varepsilon^2 - \Delta(\theta)^2|}. \tag{31}$$

Equation (30) shows both the band of the subgap states generated by diffuse scattering and the Tomasch oscillations for energies above the continuum. The positions of the maxima are determined by the condition for constructive interference of particlelike and holelike excitations with energies above the gap, $|\Delta_\parallel \sin\theta|$, reflecting from the specular surface,

$$\frac{2\sqrt{\varepsilon^2 - \Delta_\parallel^2 \sin^2\theta}}{v_f \cos\theta} D = n\pi, \quad n = 0,1,2 \ldots . \tag{32}$$

The spectral weight of the Tomasch oscillations also depends on distance from the surface. Some peaks are suppressed at special positions in the film due to spatial oscillations of the particle-hole interference amplitudes. This suppression of spectral weight is most visible for angles close to $\theta = \pi/2$ near the free surface. For example, the density of states for $\theta = 0.4\pi$ at $z = 19/20D$ shows that every second peak is suppressed.

The subgap states are bound to the surface on the length scale set by coherence length ξ_0 and decay exponentially into the bulk. However, the situation is different for thin films; the bound states extend over the entire width of the film. Figure 8 shows the total DOS averaged over the film, $N(\varepsilon) = \int dz/D \int d\Omega_{\hat{\mathbf{p}}}/4\pi N(\hat{\mathbf{p}}, z; \varepsilon)$. The spectrum is gapless over the entire energy range $\varepsilon < \Delta_0$ and is finite at $\varepsilon = 0$. The inset to Fig. 8 shows the evolution of the total DOS as a function of temperature. The gapless states fill the spectrum $\varepsilon < \Delta_0$ completely as $T \to T_c^{\text{film}}$.

At low temperatures $T \to 0$, the DOS is insensitive to temperature, and the value of the DOS at $\varepsilon = 0, 0 < N(0) < N_f$, persists above $\varepsilon = 0$. If we decrease the film thickness, the subgap states fill the gap and a transition to the normal state will occur when this process is complete. As shown in Fig. 8 the density of states is almost equal to that for the normal state over the whole energy range for $D = 0.8\xi_0$. The A to normal transition occurs for a slightly smaller film thickness.

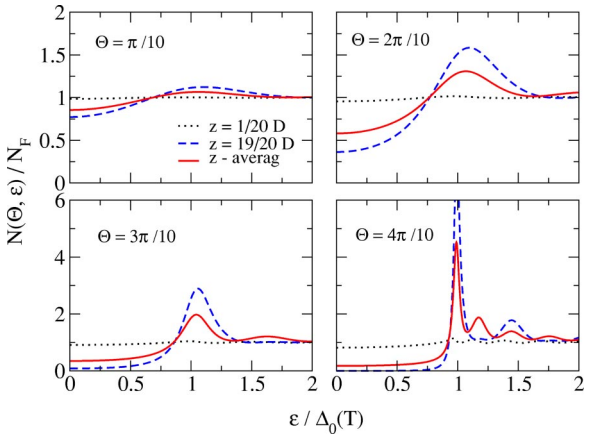

FIG. 7. The density of states in the A phase for a film of thickness $D = 4\xi_0$ at temperature $T = 0.01T_c$. The excitation energy is scaled in units of $\Delta_0(T)$, the bulk value of $\Delta_\parallel$ at temperature T.

As a consequence of the gapless spectrum the thermodynamic properties of the films of ^{3}He-A will be very different from those of bulk ^{3}He. For example, the low-temperature behavior of the specific heat vanishes exponentially in bulk ^{3}He-B for $T \ll \Delta_B$, $C_B^{\text{bulk}}(T) \to (T_c/T)^{3/2} \exp(-\Delta_0/T)$, while for bulk ^{3}He-$A$ the nodal excitations have zero energy at isolated points on the Fermi surface. The bulk density of states vanishes at the Fermi level as $N_A^{\text{bulk}}(\varepsilon \to 0) \sim \varepsilon^2$, and the specific heat exhibits a power law $C_A^{\text{bulk}} \sim (T/T_c)^3$.

The specific heat of films of superfluid ^{3}He-A is expected to have a different power-law behavior at low temperatures. The density of states is finite and nearly constant in the low-energy range above the Fermi level. As a result the specific heat will have the linear temperature dependence as $T \to 0$, just as for normal ^{3}He, except that the Sommerfeld coefficient is reduced in the superfluid film by the ratio $N(0)/N_f$.

V. THERMODYNAMIC PROPERTIES

To compute the thermodynamic properties of superfluid ^{3}He films we need a free-energy functional formulated in terms of the quasiclassical propagator and self-energies. Such a functional has been derived starting from the general Luttinger-Ward functional, formulated in terms of the full Green's function and self-energy, by eliminating the high-energy, short-wavelength intermediate states and thus computing only corrections to the ground-state energy to leading order in the small expansion parameters of Fermi-liquid theory. The conceptual formulation of this problem is discussed in detail by Rainer and Serene.[36] The formulation of a quasiclassical free-energy functional for inhomogeneous equilibrium states is similar, but there are additional technical approaches to incorporating inhomogeneities of the order parameter.[26,30,37] Our approach is similar to that of Ref. 26 and is outlined in Appendix B.

We start from the quasiclassical free energy in the weak-coupling limit expressed in terms of the quasiclassical propagator $\hat{g}(\hat{\mathbf{p}}, \mathbf{R}; \varepsilon_m)$ and order parameter $\hat{\Delta}(\hat{\mathbf{p}}, \mathbf{R})$ derived in Eq. (B16),

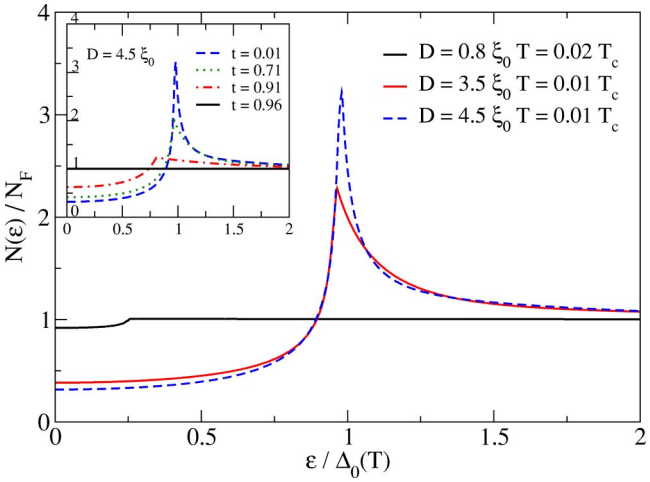

FIG. 8. The total DOS averaged over film for several film thicknesses for $T \ll T_c^{\text{film}}$. The inset shows the gapless excitations filling the gap for $t = T/T_c^{\text{film}} \to 1$.

$$\Delta\Omega[\hat{g},\hat{\Delta}] = -\frac{1}{4}\mathrm{Sp}'(\hat{\Delta}\hat{g}) + \frac{1}{2}\int_0^1 d\lambda\ \mathrm{Sp}'(\hat{\Delta}\hat{g}_\lambda). \tag{33}$$

The symbol Sp' denotes the sum over relevant variables: the volume of the ^{3}He film, position on the Fermi surface, Matsubara energies, and a trace over spin and particle-hole degrees of freedom,

$$\mathrm{Sp}'(\cdots) = N_f \int d^3R \int \frac{d\Omega_{\hat{\mathbf{p}}}}{4\pi} T\sum_m \mathrm{Tr}_4(\cdots). \tag{34}$$

There is an additional integration over the variable coupling parameter λ in Eq. (33) involving an auxiliary propagator $\hat{g}_\lambda$, which is the solution of the quasiclassical transport equation in Eq. (5), but with the self-energy scaled by λ: $\hat{\Delta} \rightarrow \hat{\Delta}_\lambda = \lambda\hat{\Delta}$. The transport equation for $\hat{g}_\lambda$ is not solved self-consistently, but with a single integration for each value of λ. Thus, $\hat{g}_\lambda$ is a function of the exact order parameter in the film. This procedure and the application of boundary conditions for computing the auxiliary propagator and the quasiclassical free energy functional are also explained in Appendix B.

Equation (33), when evaluated with the self-consistently determined propagator and order parameter in the film, gives the difference of the thermodynamic potential, $\Delta\Omega = \Omega_S - \Omega_N$, from which the change in entropy and specific heat can be calculated,

$$\Delta S(T) = -\frac{\partial\,\Delta\Omega}{\partial T}, \qquad \Delta C(T) = -T\frac{\partial^2\,\Delta\Omega}{\partial T^2}. \tag{35}$$

The normal-state free energy for ^{3}He of volume V is given by $\Omega_N(T) = E_N - V(\frac{1}{2}\gamma_N T^2)$, where E_N is the ground-state energy for normal ^{3}He and $\gamma_N = (2\pi^2/3)N_f k_B^2$ is the normal-state Sommerfeld coefficient.

The reduction of the free energy below the normal-state value represents the gain in energy due to the formation of a condensate of pairs in the film. The free energy of ^{3}He-A films in the limit of diffuse scattering by the substrate is shown in Fig. 9 for several film thicknesses. The reduction in the free energy is given by the Ginzburg-Landau form $\Delta\Omega \propto -(1 - T/T_c^{\mathrm{film}})^2$ for temperatures just below the superfluid transition temperature T_c^{film} of the film. At low temperatures the gapless excitations dominate the thermodynamics. The density of states at the Fermi energy is nonzero and approximately constant at low energies. As a result the low-temperature limit for the free energy of the superfluid state decreases as $\Omega_S - E_S = -V(\frac{1}{2}\gamma_S T^2)$, where $\gamma_S < \gamma_N$ is the Sommerfeld coefficient for the low-energy excitations of the superfluid film and E_S is the $T=0$ condensation energy.

From the numerical results shown in Fig. 9 we can calculate temperature dependence of the entropy and specific heat of the ^{3}He-A film. The results for the entropy are shown in the inset of Fig. 9. The linear temperature dependence of the entropy resulting from the gapless excitations is clearly visible.

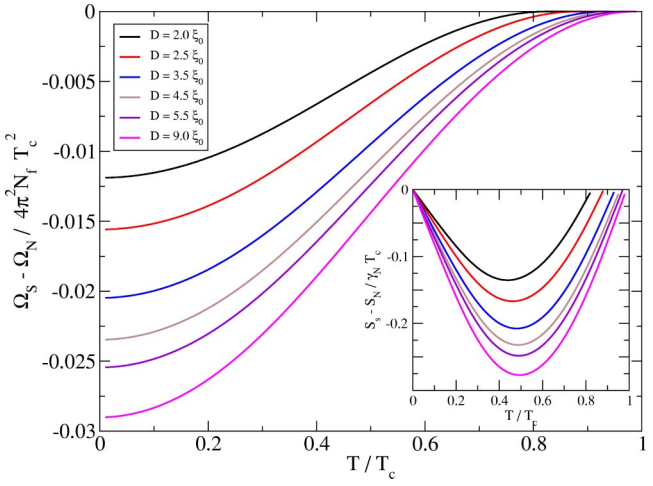

FIG. 9. Superfluid correction to the thermodynamic potential vs reduced temperature for several films of superfluid ^{3}He-A on a rough substrate. The inset shows the reduction in the entropy of the superfluid film.

Numerical calculations of the specific heat are shown in Fig. 10. These results show the decrease of the heat capacity jump at T_c^{film} with decreasing film thickness, as well as the linear temperature dependence of the specific heat resulting from the gapless excitations (see inset of Fig. 9). This behavior for ^{3}He-A films is in sharp contrast to the low-temperature heat capacity of bulk ^{3}He-A, which varies as $C_S \sim T^3$.

Results for the heat capacity jump $\Delta C(T_c^{\mathrm{film}})/\gamma_N T_c^{\mathrm{film}}$ and the Sommerfeld coefficient γ_S are summarized in Fig. 11 as a function of the film thickness D. The Sommerfeld coefficient γ_S was calculated by two independent methods. We calculated γ_S directly by numerically differentiating the tem-

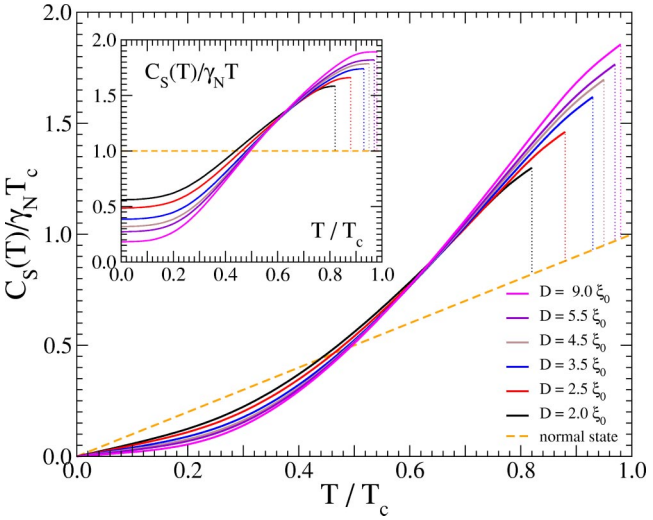

FIG. 10. The specific heat of a superfluid ^{3}He-A film as a function of reduced temperature for several film thicknesses. The inset shows the ratio $C_S(T)/C_N(T)$.

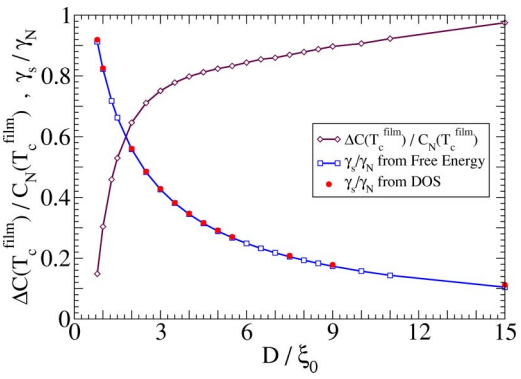

FIG. 11. Specific heat jump $\Delta C(T_c^{\rm film})/\gamma_N T_c^{\rm film}$ at $T_c^{\rm film}$ and the ratio of the low-temperature Sommerfeld coefficient, γ_S/γ_N, for the superfluid film as a function of film thickness D. For comparison, $\Delta C(T_c)/\gamma_N T_c = 1.19$ for bulk ^{3}He-A in the weak-coupling limit.

perature dependence of the superfluid free energy. We can also relate the Sommerfeld coefficient directly to the density of states at the Fermi energy, $N(0)$. Thus, $\gamma_S/\gamma_N = N(0)/N_f$. The first calculation is carried out entirely in the Matsubara formalism, while the calculation of the DOS at the Fermi level is obtained by the solving for the retarded quasiclassical propagator on the real energy axis. Both results agree and are shown in Fig. 11 and give us confidence in our numerical calculations for the propagators, free energy, entropy, and heat capacity.

VI. CONCLUSION

We have calculated the thermodynamic properties of thin films of superfluid ^{3}He in the weak-coupling limit, expected to be applicable to films at zero pressure. We calculated the phase diagram for the superfluid film, including the *AB* transition, the suppression of the superfluid transition temperature, suppression of the order parameter, the quasiparticle density of states, and thermodynamic potential. Our analysis, based on the quasiclassical method, shows a spectrum for superfluid films with gapless excitations formed by the combination of reflection by a rough substrate and Andreev scattering induced by changes in the order parameter along classical trajectories of quasiparticles. The gapless excitation spectrum depends on the film thickness and dominates the low-temperature thermodynamic potential, entropy, and specific heat.

ACKNOWLEDGMENTS

We thank Matthias Eschrig and Tomas Löfwander for helpful discussions and acknowledge support from the NSF through Grant No. DMR-9972087.

APPENDIX A: DIFFUSE SCATTERING

The boundary condition for the quasiclassical propagator at a rough surface is obtained by solving the transport equation

$$[i\varepsilon_m \hat{\tau}_3 - \hat{\mathfrak{S}}_{\rm imp}(\hat{\mathbf{p}},\mathbf{R};\varepsilon_m) - \hat{\Delta}(\hat{\mathbf{p}},\mathbf{R}), \hat{g}(\hat{\mathbf{p}},\mathbf{R};\varepsilon_m)] + i\mathbf{v}_f\cdot\boldsymbol{\nabla}\hat{g}(\hat{\mathbf{p}},\mathbf{R};\varepsilon_m) = 0 \tag{A1}$$

in the dirty layer and matching this solution to the quasiclassical propagator in the superfluid. In the limit of strong disorder within the impurity layer, $|\mathfrak{S}_{\rm imp}| \gg |\varepsilon_m|, |\Delta|$. Thus, deep in the impurity layer,

$$[\hat{\mathfrak{S}}_{\rm imp}(\hat{\mathbf{p}},\mathbf{R};\varepsilon_m), \hat{g}(\hat{\mathbf{p}},\mathbf{R};\varepsilon_m)] = 0, \tag{A2}$$

with the impurity self-energy evaluated in the Born approximation,

$$\hat{\mathfrak{S}}_{\rm imp} = \frac{1}{2\pi}\int \frac{d\Omega_{\hat{\mathbf{p}}'}}{4\pi}\tau^{-1}(\hat{\mathbf{p}},\hat{\mathbf{p}}')\,\hat{g}(\hat{\mathbf{p}}',\mathbf{R};\varepsilon_m), \tag{A3}$$

where $\tau^{-1}(\hat{\mathbf{p}},\hat{\mathbf{p}}')$ is the rate for quasiparticles to scatter from $\hat{\mathbf{p}}\to\hat{\mathbf{p}}'$ on the Fermi surface. These equations are solved by an isotropic propagator $\hat{g}_{\rm TDL}(\varepsilon_m)$, which is normalized to $\hat{g}^2_{\rm TDL} = -\pi^2\hat{1}$. This propagator is *not* the normal-state propagator for the isolated normal metal because the proximity coupling to the superfluid layer produces a "rotation" of $\hat{g}_N(\varepsilon_m)\to\hat{g}_{\rm TDL}(\varepsilon_m)$ in particle-hole space. To fix this rotation we include the leading corrections to Eq. (A2) due to spatial variations of the propagator in both the TDL and superfluid film and match the solutions at the interface. In the TDL the transport equation is

$$i\mathbf{v}_f\cdot\boldsymbol{\nabla}\hat{g}(\hat{\mathbf{p}},\mathbf{R};\varepsilon_m) = [\hat{\mathfrak{S}}_{\rm imp}(\hat{\mathbf{p}},\mathbf{R};\varepsilon_m), \hat{g}(\hat{\mathbf{p}},\mathbf{R};\varepsilon_m)]. \tag{A4}$$

Equations (A3) and (A4) are solved by expanding the propagator in a basis of Nambu matrices. For superfluid ^{3}He films in zero field the basis is limited to matrices in 2×2 particle-hole space, with the spin degrees of freedom fixed. Thus, three linearly independent matrices $\{\hat{g}_1,\hat{g}_2,\hat{g}_3\}$ are required [the identity matrix drops out of Eq. (A4)]. These matrices satisfy the algebraic relations of the Pauli matrices,

$$[\hat{g}_i,\hat{g}_j]_+ = -2\pi^2\delta_{ij}, \quad [\hat{g}_i,\hat{g}_j]_- = -2\pi\varepsilon_{ijk}\hat{g}_k. \tag{A5}$$

We choose $\hat{g}_3 = \hat{g}_{\rm TDL}$ and express the propagator in the TDL as

$$\hat{g}(\hat{\mathbf{p}},\mathbf{R};\varepsilon_m) = B_+(\hat{\mathbf{p}},\mathbf{R})\hat{g}_+(\varepsilon_m) + B_-(\hat{\mathbf{p}},\mathbf{R})\hat{g}_-(\varepsilon_m) + B_3(\hat{\mathbf{p}},\mathbf{R})\hat{g}_3(\varepsilon_m), \tag{A6}$$

where $\hat{g}_\pm = (\hat{g}_1 \pm i\hat{g}_2)/\sqrt{2}$. The linear differential equations for $\{B_3(\hat{\mathbf{p}},\mathbf{R}), B_+(\hat{\mathbf{p}},\mathbf{R}), B_-(\hat{\mathbf{p}},\mathbf{R})\}$ are easily solved with Ovchinnikov's model of forward scattering, $\tau^{-1}(\hat{\mathbf{p}},\hat{\mathbf{p}}') = 4\tau^{-1}\hat{p}_z\hat{p}_z'$ for $\hat{p}_z\hat{p}_z' > 0$; otherwise, $\tau^{-1}(\hat{\mathbf{p}},\hat{\mathbf{p}}') = 0$. Thus, quasiparticles enter the dirty layer, scatter forward towards the specular wall, and after reflection diffuse out of the TDL. The limit $d\to0, v_f\tau\to0, v_f\tau/d\to0$ corresponds to diffuse scattering by the impurity layer.

The propagator in the TDL is matched to the propagator, $\hat{g}(\hat{\mathbf{p}},0;\varepsilon_m)$, in the superfluid at the interface to the TDL. We use the same basis to express

$$\hat{g}(\hat{\mathbf{p}},0;\varepsilon_m)=\hat{g}_{\mathrm{TDL}}(\varepsilon_m)+C_+(\hat{\mathbf{p}},0)\,\hat{g}_+(\varepsilon_m)+C_-(\hat{\mathbf{p}},0)\,\hat{g}_-(\varepsilon_m). \tag{A7}$$

The coefficients of this expansion satisfy the following relations obtained by Ovchinnikov[24]:

$$C_+(\hat{\mathbf{p}},0)=0,\quad \hat{p}_z<0,\quad \int_{\hat{p}_z>0}\frac{d\Omega_{\hat{p}}}{\pi}|\hat{p}_z|C_+(\hat{\mathbf{p}},0)=0,$$

$$C_-(\hat{\mathbf{p}},0)=0,\quad \hat{p}_z>0,\quad \int_{\hat{p}_z<0}\frac{d\Omega_{\hat{p}}}{\pi}|\hat{p}_z|C_-(\hat{\mathbf{p}},0)=0. \tag{A8}$$

The propagator deep in the dirty layer is also related to the physical propagator at the boundary,

$$\hat{g}_{\mathrm{TDL}}(\varepsilon_m)=\int_{\substack{\hat{p}_z>0\\ \hat{p}_z<0}}\frac{d\Omega_{\hat{p}}}{\pi}|\hat{p}_z|\,\hat{g}(\hat{\mathbf{p}},0,\varepsilon_m). \tag{A9}$$

The boundary conditions (A7)–(A9) can be written in a compact form using the commutation relations (A5),

$$\hat{g}(\hat{\mathbf{p}},0;\varepsilon_m)-\hat{g}_{\mathrm{TDL}}(\varepsilon_m)=\frac{\mathrm{sgn}(\hat{p}_z)}{2\pi i}[\hat{g}_{\mathrm{TDL}}(\varepsilon_m),\hat{g}(\hat{\mathbf{p}},0;\varepsilon_m)]. \tag{A10}$$

This condition is solved self-consistently with Eq. (A9) for $\hat{g}_{\mathrm{TDL}}$ and $\hat{g}(\hat{\mathbf{p}},0;\varepsilon_m)$.

The boundary condition for $\hat{g}(\hat{\mathbf{p}},0;\varepsilon_m)$ can be cast into a more compact form using the Ricatti representation for the propagator $\hat{g}$. For an outgoing trajectory $\hat{p}_z>0$, Eq. (A10) is solved by

$$\hat{a}(\hat{\mathbf{p}},0)=-(i\pi-\hat{g}_{\mathrm{TDL}})^{-1}\hat{f}_{\mathrm{TDL}}. \tag{A11}$$

Thus, integration along an outgoing trajectory should start with the value of $\hat{a}$ given by the value deep in the thin dirty layer. The second Ricatti amplitude $\underline{\hat{a}}$ is known at the TDL substrate, since we integrate $\underline{\hat{a}}$ along a trajectory with $\hat{p}_z>0$ in the backward direction. Thus, Eqs. (A9) and (A11), together with $\underline{\hat{a}}(\hat{\mathbf{p}},0;\varepsilon_m)$ and the Ricatti parametrization (10), (11), are iterated until they converge to a value for $\hat{a}(\hat{\mathbf{p}},0)$.

We use the fourth-order Runge-Kutta method to numerically integrate the Ricatti equations along a classical trajectory for the Ricatti amplitudes $\hat{a}(\mathbf{p},z;\varepsilon_m)$ and $\underline{\hat{a}}(\mathbf{p},z;\varepsilon_m)$. Azimuthal symmetry for scattering in the plane of the film allows us to consider trajectories defined by θ and $\phi=0$ (Fig. 12). The integration procedure is slightly different for the *A* and *B* phases. In the case of the *A* phase we know the Riccati amplitudes at the interface with the substrate [Eq. (25)]: $\hat{a}(\theta,0;\varepsilon_m)=\underline{\hat{a}}(\theta,0;\varepsilon_m)=0$. For any trajectory we start at point 1 and integrate forward along trajectory $1-S-2$,

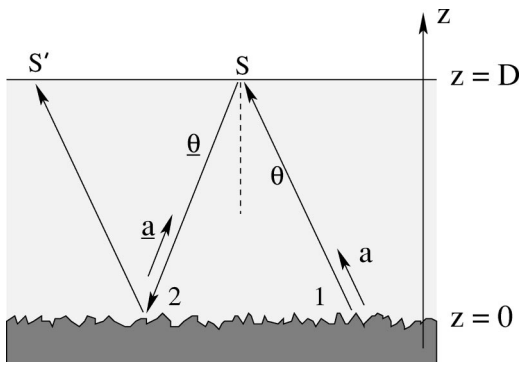

FIG. 12. Integration along classical trajectories.

with specular reflection at *S*, to obtain the amplitude $\hat{a}$. To calculate $\underline{\hat{a}}$ we integrate along the same trajectory in the reverse direction starting at point 2.

For the *B* phase we do not know the initial values of the Ricatti amplitudes anywhere. In this case we start with an initial guess for the amplitude $\hat{a}$, e.g., at the point *S*. Using Eq. (16) and inversion in the azimuthal plane we find a starting value for the amplitude $\underline{\hat{a}}$. We then integrate from *S* to 2 to obtain $\hat{a}(\theta,0;\varepsilon_m)$ and from S' to 2 to obtain $\underline{\hat{a}}(\theta,0;\varepsilon_m)$. We implement the diffuse boundary conditions at point 2 to obtain $\hat{a}(\theta,0;\varepsilon_m)$ and then integrate from 2 to S'. This gives us an updated initial value for the amplitude $\hat{a}$ (and by symmetry for $\underline{\hat{a}}$). The integration procedure is repeated until convergence is reached.

APPENDIX B: FREE-ENERGY FUNCTIONAL

We start with the Luttinger-Ward functional for the full Nambu Green's function $\hat{G}$ and self-energy $\hat{\Sigma}$,

$$\Omega[\hat{G},\hat{\Sigma}]=-\frac{1}{2}\mathrm{Sp}\{\hat{\Sigma}\hat{G}+\ln(-\hat{G}_0^{-1}+\hat{\Sigma})\}+\Phi[\hat{G}], \tag{B1}$$

where

$$\mathrm{Sp}\{\cdots\}=T\sum_{\varepsilon_m}\int d^3R\int\frac{d^3p}{(2\pi)^3}\mathrm{Tr}_4\{\cdots\}, \tag{B2}$$

$\hat{\Sigma}(\mathbf{p},\mathbf{R};\varepsilon_m)$ is the self-energy, and $\hat{G}_0^{-1}(\mathbf{p},\mathbf{R};\varepsilon_m)=i\varepsilon_m\hat{\tau}_3-\xi_0(\mathbf{p})\hat{1}$ is the inverse Green's function for a noninteracting reference system of bare ^{3}He. The stationarity condition with respect to the Green's function,

$$\frac{\delta\Omega}{\delta\hat{G}^{\mathrm{tr}}}=0\rightsquigarrow\hat{\Sigma}=\hat{G}_{\mathrm{skel}}[\hat{G}]=2\frac{\delta\Phi[\hat{G}]}{\delta\hat{G}^{\mathrm{tr}}}, \tag{B3}$$

relates the functional $\Phi[\hat{G}]$ to the self-energy via the skeleton expansion for the self-energy, while the stationarity condition with respect to the self-energy,

$$\frac{\delta\Omega}{\delta\widehat{\Sigma}^{\rm tr}}=0\rightsquigarrow\widehat{G}^{-1}=\widehat{G}_0^{-1}-\widehat{\Sigma}, \tag{B4}$$

gives Dyson's equation for the Nambu propagator. These equations provide a starting point for deriving the Fermi-liquid theory for superfluid ^{3}He. In particular, the leading-order expansion of Dyson's equation in the small parameters of Fermi-liquid theory can be transformed into Eilenberger's transport equation [Eq. (5)] for the quasiclassical propagator.

In order to derive a free-energy functional of the quasiclassical propagator $\widehat{g}$ and quasiclassical self-energy

$$\widehat{\mathfrak{S}}(\hat{\mathbf{p}},\mathbf{R};\varepsilon_m)\equiv a[\,\widehat{\Sigma}(p_f\hat{\mathbf{p}},\mathbf{R};\varepsilon_m)-\widehat{\Sigma}_N]\,\hat{\tau}_3, \tag{B5}$$

we remove the normal-state stationary point $(\widehat{G}_N,\widehat{\Sigma}_N)$ from the Luttinger-Ward functional [Eq. (B1)] by defining $\Delta\widehat{\Sigma}=\widehat{\Sigma}-\widehat{\Sigma}_N$, $\Delta\widehat{G}=\widehat{G}-\widehat{G}_N$ and introducing the subtracted functional

$$\begin{aligned}\Delta\Omega[\,\widehat{G},\Delta\widehat{\Sigma}]&=\Omega[\,\widehat{G},\widehat{\Sigma}]-\Omega[\,\widehat{G}_N,\widehat{\Sigma}_N]\\&=-\frac{1}{2}\mathrm{Sp}\{\,\Delta\widehat{\Sigma}\,\widehat{G}+\ln(-\widehat{G}_N^{-1}+\,\Delta\widehat{\Sigma})\\&\quad-\ln(-\widehat{G}_N^{-1})\}+\,\Delta\Phi[\,\widehat{G}\,],\end{aligned} \tag{B6}$$

which has as inputs the normal-state propagator $\widehat{G}_N=(\widehat{G}_0^{-1}-\widehat{\Sigma}_N)^{-1}$ and self-energy $\widehat{\Sigma}_N$ rather than the bare propagator. The subtracted Φ functional

$$\Delta\Phi[\,\widehat{G}\,]=\Phi[\,\widehat{G}\,]-\Phi[\,\widehat{G}_N]-\frac{1}{2}\mathrm{Sp}\{\,\widehat{\Sigma}_N(\,\widehat{G}-\widehat{G}_N)\} \tag{B7}$$

is confined to the low-energy region of phase space since pairing corrections to the normal-state propagator contribute only in the low-energy region $k_BT_c\ll E_f$. The diagrammatic perturbation expansion for $\Delta\Phi$ can be reorganized as an asymptotic expansion in the small parameters of Fermi-liquid theory[36] that is formally an expansion in the number of low-energy propagator lines.

To convert Eq. (B6) to a functional of the quasiclassical propagator and self-energy we integrate out the momentum dependence normal to the Fermi surface over a region of momentum space near the Fermi surface, $|\xi_{\mathbf{p}}|<\varepsilon_c$. The low-energy self-energy is a slowly varying function of $\xi_{\mathbf{p}}$ and can be evaluated with $\mathbf{p}=p_f\hat{\mathbf{p}}$. Thus, the term $\Delta\widehat{\Sigma}\,\widehat{G}$ in Eq. (B6) is ξ_p integrated to give

$$\begin{aligned}\mathrm{Sp}\{\Delta\widehat{\Sigma}\,\widehat{G}\}&\Rightarrow\mathrm{Sp}'\{\widehat{\mathfrak{S}}\,\widehat{g}\}\\&\equiv N_fT\sum_m\int d^3R\int\frac{d\Omega_{\hat{\mathbf{p}}}}{4\pi}\\&\quad\times\mathrm{Tr}_4[\,\widehat{\mathfrak{S}}(\hat{\mathbf{p}},\mathbf{R};\varepsilon_m)\,\widehat{g}\,(\hat{\mathbf{p}},\mathbf{R};\varepsilon_m)].\end{aligned} \tag{B8}$$

To integrate the ln functional we introduce an auxiliary functional defined by introducing a variable coupling constant for the self-energy and Φ functional: $\Delta\widehat{\Sigma}\rightarrow\Delta\widehat{\Sigma}_\lambda\equiv\lambda\,\Delta\widehat{\Sigma}$ and $\Delta\Phi\rightarrow\Delta\Phi_\lambda\equiv\lambda\,\Delta\Phi$. Thus, the auxiliary functional is

$$\begin{aligned}\Delta\Omega_\lambda[\,\widehat{G},\Delta\widehat{\Sigma}_\lambda]&=-\frac{1}{2}\mathrm{Sp}\{\,\Delta\widehat{\Sigma}_\lambda\,\widehat{G}+\ln(-\widehat{G}_N^{-1}+\,\Delta\widehat{\Sigma}_\lambda)\\&\quad-\ln(-\widehat{G}_N^{-1})\}+\lambda\,\Delta\Phi[\,\widehat{G}\,].\end{aligned} \tag{B9}$$

The stationarity conditions with respect to $\widehat{G}$ and $\Delta\widehat{\Sigma}_\lambda$ give a new equation for an auxiliary propagator, $\widehat{G}_\lambda^{-1}\equiv\widehat{G}_N^{-1}-\Delta\widehat{\Sigma}_\lambda$. The auxiliarly functional can be $\xi_{\mathbf{p}}$ integrated after first differenting with respect to the coupling parameter, then carrying out the $\xi_{\mathbf{p}}$ integration to obtain

$$\frac{\partial\,\Delta\Omega_\lambda}{\partial\lambda}=-\frac{1}{2}\mathrm{Sp}'\{\widehat{\mathfrak{S}}\,\widehat{g}\}+\frac{1}{2}\mathrm{Sp}'\{\widehat{\mathfrak{S}}\,\widehat{g}_\lambda\}+\,\Delta\Phi[\,\widehat{g}\,], \tag{B10}$$

where

$$\widehat{g}_\lambda(\hat{\mathbf{p}},\mathbf{R};\varepsilon_m)=\frac{1}{a}\int_{-\varepsilon_c}^{+\varepsilon_c}d\xi_{\mathbf{p}}\,\hat{\tau}_3\,\widehat{G}_\lambda(\mathbf{p},\mathbf{R};\varepsilon_m) \tag{B11}$$

is the quasiclassical auxiliary propagator. We can integrate Eq. (B10) with respect to the coupling constant. Since $\Delta\Omega_{\lambda=0}=0$ and $\Delta\Omega_{\lambda=1}=\Delta\Omega$, we obtain the desired free-energy functional in terms of the quasiclassical propagator $\hat{g}$ and self-energy $\widehat{\mathfrak{S}}$,

$$\Delta\Omega[\,\widehat{g},\widehat{\mathfrak{S}}]=\frac{1}{2}\int_0^1 d\lambda\,\mathrm{Sp}'\{\widehat{\mathfrak{S}}(\,\widehat{g}_\lambda-\widehat{g})\}+\,\Delta\Phi[\,\widehat{g}\,]. \tag{B12}$$

The stationarity conditions for the subtracted free-energy functional reduce to the quasiclassical transport equation and self-energy expansion obtained from the asymptotic expansion of the Φ functional,

$$[\,i\varepsilon_m\hat{\tau}_3-\widehat{\mathfrak{S}},\widehat{g}\,]+i\mathbf{v}_f\cdot\boldsymbol{\nabla}\,\widehat{g}=0,\quad\widehat{\mathfrak{S}}=2\frac{\delta\,\Delta\Phi[\,\widehat{g}\,]}{\delta\widehat{g}^{\rm tr}}. \tag{B13}$$

These equations are supplemented by boundary conditions for the propagator $\widehat{g}$ which describe the effects of scattering by a surface or interface.

The auxiliary propagator $\widehat{g}_\lambda$ is a functional of the exact quasiclassical self-energy and is obtained by solving the quasiclassical transport equation with $\widehat{\mathfrak{S}}\rightarrow\lambda\,\widehat{\mathfrak{S}}$,

$$[\,i\varepsilon_m\hat{\tau}_3-\lambda\,\widehat{\mathfrak{S}},\widehat{g}_\lambda]+i\mathbf{v}_f\cdot\boldsymbol{\nabla}\,\widehat{g}_\lambda=0. \tag{B14}$$

This auxiliary transport equation is solved once (not self-consistently) for each value of λ with $\widehat{\mathfrak{S}}$ as a predetermined

input function. The diffuse boundary condition for $\hat{g}_\lambda$ is given by Eq. (A10) with $\hat{g}_{\rm TDL}$ fixed by the self-consistently determined solution of the quasiclassical equations and boundary condition for $\lambda = 1$.

A further simplification for $\Delta\Omega$ is possible in the weak-coupling limit when the self-energy is purely off diagonal and given by the order parameter $\hat{\mathfrak{S}} = \hat{\Delta}$. The self-consistency equation

$$\hat{\Delta} = 2\frac{\delta\Delta\Phi[\hat{g}]}{\delta\hat{g}^{\rm tr}} \tag{B15}$$

can be used to evaluate $\Delta\Phi[\hat{g}] = \frac{1}{4}\,\mathrm{Sp}'\{\hat{\Delta}\hat{g}\}$. The resulting free energy reduces to

$$\Delta\Omega = \frac{1}{2}\int_0^1 d\lambda\ \mathrm{Sp}'\left\{\hat{\Delta}\left(\hat{g}_\lambda - \frac{1}{2}\hat{g}\right)\right\}. \tag{B16}$$

[1] D. Vollhardt and P. Wölfle, *The Superfluid Phases of Helium 3* (Taylor & Francis, London, 1990).
[2] A. Sachrajda, R.F. Harris-Lowe, J.P. Harrison, R.R. Turkington, and J.G. Daunt, Phys. Rev. Lett. **55**, 1602 (1985).
[3] J.C. Davis, A. Amar, J.P. Pekola, and R.E. Packard, Phys. Rev. Lett. **60**, 302 (1988).
[4] J.G. Daunt, R.F. Harris-Lowe, J.P. Harrison, A. Sachrajda, S.C. Steel, R.R. Turkington, and P. Zawadski, J. Low Temp. Phys. **70**, 547 (1988).
[5] S.C. Steel, J.P. Harrison, P. Zawadski, and A. Sachrajda, J. Low Temp. Phys. **95**, 759 (1994).
[6] M.R. Freeman, R.C. Germain, E.V. Thuneberg, and R.C. Richardson, Phys. Rev. Lett. **60**, 596 (1988).
[7] J. Xu and B.C. Crooker, Phys. Rev. Lett. **65**, 3005 (1990).
[8] T. Kawae, M. Kubota, Y. Ishimoto, S. Miyawaki, O. Ishikawa, T. Hata, and T. Kodama, J. Low Temp. Phys. **111**, 917 (1998).
[9] A. Schechter, R.W. Simmonds, R.E. Packard, and J.C. Davis, Nature (London) **396**, 554 (1998).
[10] V. Ambegaokar, P. de Gennes, and D. Rainer, Phys. Rev. A **9**, 2676 (1975).
[11] L. Kjäldman, J. Kurkijärvi, and D. Rainer, J. Low Temp. Phys. **33**, 577 (1987).
[12] Y-H. Li and T-L. Ho, Phys. Rev. B **38**, 2362 (1988).
[13] A.L. Fetter and S. Ullah, J. Low Temp. Phys. **70**, 515 (1988).
[14] G. Eilenberger, Z. Phys. **214**, 195 (1968).
[15] A.I. Larkin and Y.N. Ovchinnikov, Sov. Phys. JETP **28**, 1200 (1969).
[16] G.M. Eliashberg, Zh. Éksp. Teor. Fiz **61**, 1254 (1971) [Sov. Phys. JETP **34**, 668 (1972)].
[17] L.J. Buchholtz and D. Rainer, Z. Phys. B **35**, 151 (1979).
[18] L.J. Buchholtz, Phys. Rev. B **33**, 1579 (1986).
[19] L.J. Buchholtz, Phys. Rev. B **44**, 4610 (1991).
[20] W. Zhang, J. Kurkijärvi, and E.V. Thuneberg, Phys. Rev. B **36**, 1987 (1987).
[21] E. Thuneberg, M. Fogelström, and J. Kurkijärvi, Physica B **178**, 176 (1992).
[22] K. Nagai, in *Quasiclassical Methods in Superconductivity and Superfluidity*, edited by D. Rainer and J. A. Sauls (Verditz, Bayreuth, Germany, 1996).
[23] Y. Nagato, M. Yamamoto, and K. Nagai, J. Low Temp. Phys. **110**, 1135 (1998).
[24] Y.N. Ovchinnikov, Sov. Phys. JETP **29**, 853 (1969).
[25] N.B. Kopnin, P.I. Soininen, and M.M. Salomaa, J. Low Temp. Phys. **85**, 267 (1991).
[26] J.W. Serene and D. Rainer, Phys. Rep. **101**, 221 (1983).
[27] Y. Nagato, K. Nagai, and J. Hara, J. Low Temp. Phys. **93**, 33 (1993).
[28] M. Eschrig, J.A. Sauls, and D. Rainer, Phys. Rev. B **60**, 10 447 (1999).
[29] M. Eschrig, Phys. Rev. B **61**, 9061 (2000).
[30] E. Thuneberg, J. Kurkijärvi, and D. Rainer, Phys. Rev. B **29**, 3913 (1984).
[31] F. Culetto, G. Kieselmann, and D. Rainer, in *Proceedings of the 17th International Conference on Low Temperature Physics, LT-17*, edited by U. Eckern, A. Schmid, and W. Weber (Elsevier Science, Amsterdam, 1984), p. 1027.
[32] D.L. Stein and M.C. Cross, Phys. Rev. Lett. **42**, 504 (1979).
[33] H. Kawamura, Phys. Rev. Lett. **82**, 964 (1999).
[34] Y. Nagato and K. Nagai, Physica B **248-288**, 269 (2000).
[35] D. Rainer, J.A. Sauls, and D. Waxman, Phys. Rev. B **54**, 10 094 (1996).
[36] D. Rainer and J.W. Serene, Phys. Rev. B **13**, 4745 (1976).
[37] L. Buchholtz, M. Palumbo, D. Rainer, and J.A. Sauls, J. Low Temp. Phys. **101**, 1079 (1995).

[38] Rotational symmetry is broken, so to be precise we consider superfluid films in which rotational symmetry about the $\hat{\mathbf{z}}$ axis is preserved under joint rotation of the spin and orbital degrees of freedom up to an overall gauge transformation.